ACS OMEGA

http://pubs.acs.org/journal/acsodf

Article

Rapid In Vitro Quantification of a Sensitized Gadolinium Chelate via Photoinduced Triplet Harvesting

James A. Tranos,[▽] Ayesha Das,[▽] Jin Zhang, Sonia Hafeez, Georgios N. Arvanitakis, Stuart A. J. Thomson, Suleiman Khan, Neelam Pandya, Sungheon Gene Kim, and Youssef Z. Wadghiri*

Cite This: *ACS Omega* 2023, 8, 2907−2914

Read Online

ACCESS | Metrics & More | Article Recommendations | Supporting Information

ABSTRACT: Gadolinium (Gd) based contrast agents (GBCAs) are widely used in magnetic resonance imaging (MRI) and are paramount to cancer diagnostics and tumor pharmacokinetic analysis. Accurate quantification of gadolinium concentration is essential to monitoring the biodistribution, clearance, and pharmacodynamics of GBCAs. However, current methods of quantifying gadolinium in blood or plasma (biological media) are both low throughput and clinically unavailable. Here, we have demonstrated the use of a sensitized gadolinium chelate, Gd[DTPA-cs124], as an MRI contrast agent that can be used to measure the concentration of gadolinium via luminescence quantification in biological media following transmetalation with a terbium salt. Gd[DTPA-cs124] was synthesized by conjugating carbostyril-124 (cs124) to diethylenetriaminepentaacetic acid (DTPA) and chelating to gadolinium. We report increases in both stability and relaxivity compared to the clinically approved analog Gd[DTPA] (gadopentetic acid or Magnevist). In vivo MRI experiments were conducted using C57BL6 mice in order to further illustrate the performance of Gd[DTPA-cs124] as an MRI contrast agent in comparison to Magnevist. Our results indicate that similar chemical modification to existing clinically approved GBCA may likewise provide favorable property changes, with the ability to be used in a gadolinium quantification assay. Furthermore, our assay provides a straightforward and high-throughput method of measuring gadolinium in biological media using a standard laboratory plate reader.

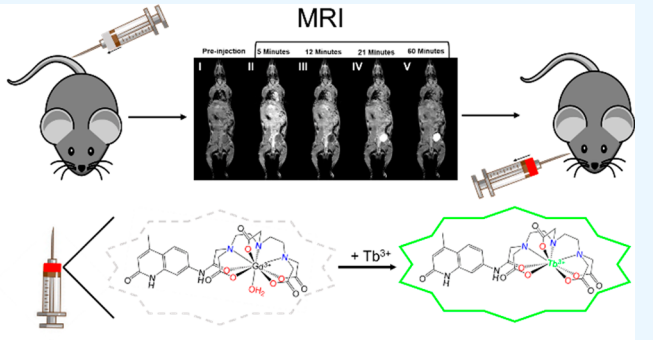

INTRODUCTION

Gadolinium (Gd) based contrast agents (GBCAs) are widely used in magnetic resonance imaging (MRI) and are especially important for early diagnoses of diseases such as cancer.[1] By measuring contrast delivery and clearance to and from tumors, the use of GBCAs extends to grading tumors and assessing treatment response.[2,3] In this context, pharmacokinetic modeling of MRI signal changes can be used to estimate GBCA concentration in tissue, providing quantitative measurements of the tumor microcirculation environment.[4,5] However, accurate measurement of GBCA concentration using dynamic contrast-enhanced MRI remains challenging due to uncertainties in multiple factors such as: the arterial input function, GBCA relaxivity in tissue, the longitudinal relaxation rate of tissue, and radiofrequency coil in homogeneities.[3] For this reason, secondary methods of measuring GBCA concentrations can be especially useful.

A potential solution to this issue is to use a bimodal MRI contrast agent such that incorporation of an internal fluorophore can be used to estimate of the amount of GBCA in a tissue sample. A sensitized ligand, namely, diethylenetriaminepentaacetic acid conjugated to carbostyril-124 (DTPA-cs124), has been studied as an optical probe where DTPA-cs124 has been used to significantly increase the long-lived fluorescence properties of lanthanide metals with low-lying resonant energy levels.[6] For some lanthanides, such as terbium (Tb) or europium (Eu), the energy absorbed by the sensitized ligand is sufficient to be transferred to the central lanthanide ion, which will then emit photons at the characteristic emission wavelength(s) for that lanthanide. We refer to this process as photoinduced triplet harvesting. In the case of gadolinium, however, the energy of the ligand triplet is typically insufficient to excite electrons of this metal, and the triplet will eventually return to the ground state via nonradiative decay.[7]

Such a photoinduced triplet harvesting (PTH) technique was used by Russell et al.[8] to detect nonluminescent metals, for

Received: August 7, 2022
Accepted: November 18, 2022
Published: January 9, 2023

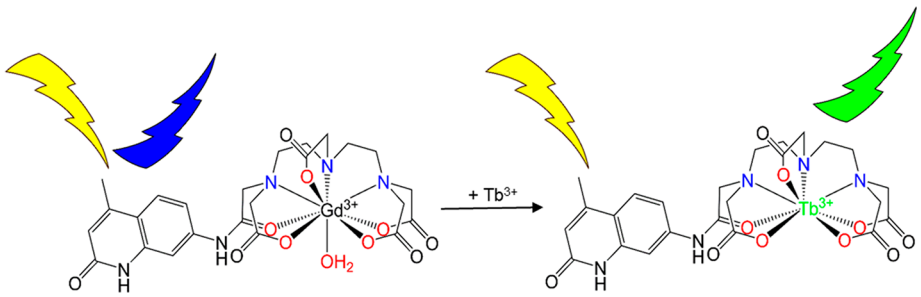

Figure 1. Mechanism of the transmetalation assay response to free aqueous Tb^{3+}. Following excitation at 330 nm, the gadolinium complex is shown emitting blue light (365 nm) from the carbostyril-124 moiety, and the terbium complex is shown emitting green light (545 nm) from the terbium ion due to intramolecular energy transfer between carbostyril-124 and Tb^{3+} following the transmetalation reaction.

instance, gadolinium, using a sensitized chelate, namely, Gd[DTPA-cs124], as an energy donor and Tb-DTPA as an energy acceptor. When the two compounds (Gd[DTPA-cs124] and Tb-DTPA) are sufficiently close, energy transfer by exchange interaction occurs, a process also known as Förster resonance energy transfer (FRET).[9,10] In this system, emission from the acceptor (Tb-DTPA), particularly at 545 nm, is quantitatively related to the concentration of gadolinium. However, amino polycarboxylate ligands, such as DTPA-cs124, favor binding to lanthanides with increasing atomic number[11] such that Tb could displace Gd from the Gd[DTPA-cs124] complex and compromise the accuracy of the measured concentration of gadolinium when using the FRET method. Alternatively, an intentional metal displacement assay between gadolinium and terbium can be utilized to transform an otherwise nonluminescent complex into a long-lived, highly luminescent species, thereby offering fluorescence quantification as a secondary method to infer the concentration of gadolinium (Figure 1).

Hence, the purpose of this study is to explore Gd[DTPA-cs124] as an MRI contrast agent, as well as its effectiveness for quantifying gadolinium in various biological media.

MATERIALS AND METHODS

A detailed synthetic scheme for the syntheses of Gd[DTPA-cs124] and Tb[DTPA-cs124] is supplied in the Supporting Information.

Standard Curves for the Quantification of Gd[DTPA-cs124]. All fluorescence measurements were performed on a Biotek H1MF plate reader. Absorbance measurements were acquired at 330 nm, and fluorescence measurements were acquired at 545 nm following excitation at 330 nm. All measurements were performed in triplicate. Fluorescence measurements were performed using a 100 μs read delay and an integration time of 1900 μs. Standard curves were obtained for human blood (5%), human plasma (5%), mouse blood (5%), and 100 mM *N*-methylglucosammonium acetate (MGAA) buffer. Human plasma and blood were obtained from the NYU Blood Center. Mouse blood was obtained from four- to six-week-old C57/BL6 mice at the time of perfusion. Standard curves were obtained by serially diluting a 1 mM Gd[DTPA-cs124] solution in 5% medium (buffer, human blood, human plasma, or mouse blood) containing a 1 mM $Tb(NO_3)_3$ ICP-MS standard solution. Assay solutions were covered and shaken at room temperature for 1 h to enable transmetalation prior to measurement.

Chelate Stability Measurements. All measurements were taken on a Bruker Minispec instrument at 60 MHz following a modified protocol described by Laurent et al.[12,13] The following commercial GBCAs were individually prepared: gadobutrol (Gadovist, Germany, Bayer), gadoteric acid (Dotarem, France, Guerbet), gadoteridol (Prohance, Italy, Bracco), gadoxetic acid (Eovist, Germany, Bayer), gadopentetic acid (Magnevist, Germany, Bayer), gadodiamide (Omniscan, United States, GE Healthcare), gadofosveset (Ablavar, United States, Lantheus), and gadobenic acid (Multihance, Italy, Bracco). All solutions and vessels were warmed to 37.5 °C prior to reaction and measurement. The experiment was initiated by adding 125 μL of aqueous $ZnCl_2$ to an NMR tube containing 250 μL of phosphate buffer solution (pH 7.4, divalent metal-free) and 125 μL of the GBCA being analyzed. The final concentrations of GBCA and $ZnCl_2$ were 2.5 mM, and the final concentration of phosphate buffer was 10 mM. Initial measurements were acquired within 1 min of adding $ZnCl_2$, shaking, and sealing the tube. The same conditions were replicated for Gd[DTPA-cs124]. Using an inversion recovery sequence, repetitive T_1 measurements were performed every 6 h at 37.5 °C for each sample for a total of 96 h, and all GBCAs were measured in triplicate. From the T_1 values acquired in the stability assay, R_1 values at each time point were calculated, normalized against the R_1 value of each GBCA at 2.5 mM, and plotted as a function of time. The stability ratio was calculated for each GBCA by taking the ratio of the average measurement at 96 h over the initial measurement at 0 h.

Relaxivity Analysis. Solutions of Gd[DTPA-cs124], gadolinium nitrate standard solution, and commercially available GBCAs (gadobutrol, gadoteric acid, gadoteridol, gadoxetic acid, gadopentetic acid, gadodiamide, gadofosveset, and gadobenic acid) were diluted in triplicate to concentrations of 2.5, 2.0, 1.5, 1.0, and 0.5 mM, in NMR tubes. T_1 values for each sample were measured on a 60 MHz Bruker mini-spectrometer at 37.5 °C using a T_1 inversion recovery sequence. For each gadolinium-based analyte, the T_1 value at each concentration was used to solve for the corresponding R_1 value, which was plotted against concentration and fitted using a linear regression in GraphPad Prism 9.0. The slope of this linear fit was reported in Table 1, as the relaxivity (r_1) for each GBCA. Additionally, the relaxivity for each GBCA, normalized by its corresponding hydration factor (q), was plotted against its calculated molecular weight and fit using a linear regression in GraphPad Prism 9.0.

In Vivo Experiments. All procedures and experiments were performed in accordance with NIH guidelines under approval by the Institutional Animal Care and Use Committee

https://doi.org/10.1021/acsomega.2c05040
ACS Omega 2023, 8, 2907−2914

Table 1. Stability and Relaxivity Properties of Investigated Contrast Media[a]

analyte	stability index	r_1 (L mmol^{-1} s^{-1} q^{-1})	molecular weight (Da)[b]
Gd^{3+}·9 H_2O	-[c]	0.90 ± 0.03[d]	319.38
gadopentetic acid	0.585 ± 0.019	3.83 ± 0.04	563.57
gadoteric acid	0.971 ± 0.019	3.00 ± 0.04	575.65
gadoteridol	0.991 ± 0.009	3.09 ± 0.06	576.7
gadodiamide	0.474 ± 0.029	3.75 ± 0.08	591.68
gadobutrol	0.998 ± 0.002	3.63 ± 0.31	622.73
gadobenic acid	0.576 ± 0.004	4.08 ± 0.01	683.72
gadoxctic acid	0.909 ± 0.018	5.08 ± 0.15	697.75
Gd[DTPA-csl24]	0.676 ± 0.015	5.09 ± 0.02	720.77
gadofosveset[e]	-	5.46 ± 0.16	906.91

[a]Magnetic resonance imaging properties of various GBCA. Stability indices were calculated from the competitive cation assay summarized in Figure 4. Relaxivity measurements, normalized to the hydration factor (q), were performed at 60 MHz and 37.5 °C at concentrations between 0.5 and 2.5 mM. Molecular weights are included to show the positive linear correlation to r_1. [b]The reported molecular weights account for the mass of the monohydrated species for all gadolinium chelates and that of the nonahydrated species for Gd^{3+}. [c]Stability data cannot be acquired for free Gd^{3+}, as $GdPO_4$ precipitation is nearly instantaneous. [d]The relaxivity of Gd^{3+} is normalized to a hydration factor of 9. [e]Measurements for gadofosveset were performed in its free aqueous state unbound to albumin.

(IACUC) of the NYU Grossman School of Medicine and the Weill Cornell Medical Center.

Magnetic Resonance Imaging. Four- to six-week-old C57/BL6 mice were used for the MRI experiments. A 3D T_1-weighted FLASH sequence with a flip angle (FA) of 15°, an echo time (TE) of 3 ms, a repetition time (TR) of 16 ms, and a matrix size of 128 × 128 × 64 was used to image the whole mouse body in less than 2.2 min per data set, and was repeated 40 times over approximately 90 min using respiratory gating. To illustrate the in vivo contrast enhancement and qualitative biodistribution of Gd[DTPA-cs124], a bolus of Gd[DTPA-cs124] was injected at a dose of 0.1 mmol kg^{-1} via a tail vein catheter after the acquisition of the first 3D image (n = 3). The same imaging protocol was acquired in another animal serving as a reference with an injection of a clinical GBCA, Gd-DTPA (gadopentetic acid, or Magnevist) at the same dose (n = 1).

Transmetalation Assay to Measure Plasma Clearance. Four- to six-week-old C57/BL6 mice (n = 5) were used for the quantitative analysis of the plasma clearance. Mice were administered a bolus injection of 0.1 mmol kg^{-1} Gd[DTPA-cs124] via tail vein cannulation. Injection volumes ranged between 90 and 100 μL depending on body weight. Eight 10 μL retro orbital (RO) blood samples were obtained from each mouse at various time points up to 2 h post injection via a graduated heparinized blood capillary. Blood samples were diluted into 90 μL of 30 U mL^{-1} meparin in 100 mM MGAA buffer (pH 6.5), affording a total volume of 100 μL of a 10× diluted blood sample. To these dilute blood samples was added an additional 100 μL of a 2 mM $Tb(NO_3)_3$ ICP-MS solution diluted in 100 mM MGAA buffer (pH = 6.5), affording a final volume of 200 μL containing 1 mM Tb solution and a 20× diluted blood sample containing an unknown amount of Gd[DTPA-cs124]. This assay solution was allowed to undergo transmetalation at room temperature, covered, for 1 h with shaking. After 1 h, an aliquot of 100 μL was used for PTH measurements.

RESULTS AND DISCUSSION

Various approaches have been explored in an attempt to reliably quantify the concentration of chelated gadolinium, with NMR relaxometry being a predominant method of choice in the literature.[14,15] This can likely be attributed to the basic principle shared by MRI and NMR instruments, where preliminary testing can be performed using benchtop NMR mini-spectrometers or high-field NMR spectrometers commonly available in chemistry departments. This is particularly practical for translation to clinical MRI scanners. Electron spin resonance (ESR) spectroscopy, a closely related method, has also been explored as a nondestructive method to measure clinically approved GBCAs within concentrations of 50 mM.[16] However, all of these methods remain inadequate for the sensitivity range and relevant concentrations typically encountered in clinical settings.

On the other hand, ICP-MS has remained the gold-standard for quantifying the concentration of gadolinium due to its high sensitivity for detecting metals at exceptionally low concentrations.[17,18] Remarkably, this analytical method is highly robust and can be performed on any type of sample irrespective of its composition due to the destructive sample preparation required for this modality.[19] Despite its high sensitivity, this specialized method has not gained widespread use in clinical studies.[20] This may be attributed to its prohibitive cost and its availability being limited to specialized laboratories.[21] Alternatively, total reflection X-ray Fluorescence (TRXF) has also been explored, holding great promise for its high reproducibility in quantifying gadolinium in blood samples following an MRI scan.[22] However, this analytical modality currently suffers from the same lack of accessibility as ICP-MS in clinical settings. To this effect, our motivation to develop a fluorescence-based approach was driven by the widespread use of optical plate readers in standard biological laboratories. Hence, using a bimodal contrast agent with fluorescent properties becomes an appealing method to quantify the concentration of gadolinium in blood.

Fluorescence. Fluorescence lifetime plots were acquired at an excitation wavelength of 330 nm for DTPA-cs124 (Supporting Figure 5), Gd[DTPA-cs124] (Figure 2A), and Tb[DTPA-cs124] (Figure 2B). The fluorescence lifetimes (τ ± standard deviation, defined as the time for the fluorescence signal to decay to e^{-1} of the maximum fluorescence intensity) were 0.50 ± 0.07, 0.44 ± 0.02, and 1481 ± 1.0 μs, respectively.

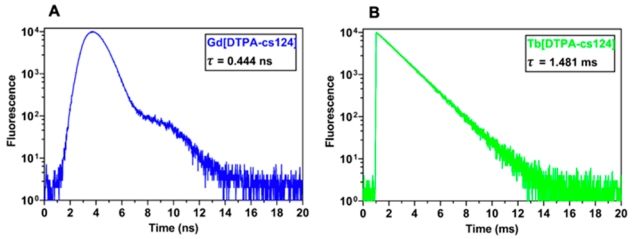

Figure 2. Fluorescence lifetime plots of (A) Gd[DTPA-cs124] and (B) Tb[DTPA-cs124], including the fluorescence lifetime (τ). Note that the Tb chelate exhibits a 10^6× increase in emission lifetime properties.

https://doi.org/10.1021/acsomega.2c05040
ACS Omega 2023, 8, 2907−2914

A variety of approaches to quantify the gadolinium concentration with fluorescence as a second modality have been synthesized and reported in the literature. This includes liposomal gadolinium-based agents tagged with rhodamine or Prussian Blue, Cy5.5,[23−25] as well as quantum dot-functionalized probes.[26] However, in the above-mentioned references, the investigators did not utilize the multimodal contrast agents to actually quantify their concentrations. Additionally, another transmetalation assay using a luminescent europium chelate for the quantification of various GBCAs in urine samples has been designed.[11] Though the micromolar limit of detection for this probe is remarkable, the use of this europium-based assay is limited in its sensitivity from 1 to 150 μM depending on the GBCA. This would be inadequate for the assessment of blood samples containing GBCAs within the submicromolar range. Unlike our method, this europium-based probe relies on luminescence quenching to quantify gadolinium, a process that can be difficult to control given the complex endogenous metallic profile of blood. In the context of DTPA-cs124, the use of its europium chelate would not be ideal given its lower quantum yield compared to Tb[DTPA-cs124] (Supplemental Figure 9). In our assay, since gadolinium is of a higher atomic number than europium and therefore less likely to transmetalate gadolinium, we could not substitute terbium with europium.[11]

In Vitro Analysis. Standard curves of quantification were acquired for serial dilutions of Gd[DTPA-cs124] in aqueous buffer, 5% human plasma, 5% human blood, and 5% mouse blood (Supporting Figure 6) in the presence of 1 mM Tb^{3+} (Figure 3). The limit of detection of Gd[DTPA-cs124] was

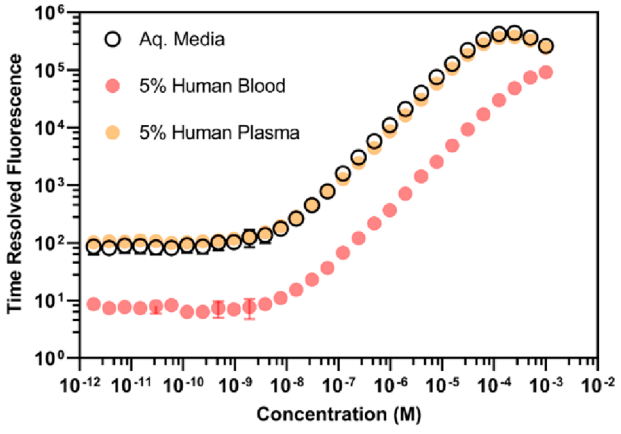

Figure 3. Standard curves for quantifying Gd[DTPA-cs124] via a transmetalation assay. Measurements were performed in an aqueous medium, 5% human plasma, and 5% human blood.

calculated in various media as the lowest concentration that could be detected based on a signal that was three standard deviations above the noise floor.[27] The resulting limits of detection for Gd[DTPA-cs124] in each media were as follows: 0.46 nM for aqueous buffer, 0.43 nM for 5% human plasma, 3.02 nM for 5% human blood, and 148.67 nM for 5% mouse blood. Using a Wilcoxon signed rank test, the limits of detection between aqueous buffer and human plasma were not significant (W = 252, p = 0.20). However, the limits of detection between aqueous buffer and human blood (W = 0, p < 0.001) as well as those between human plasma and human blood (W = 0, p < 0.001) were significantly different.

We designed an analytical assay that relied on the metal displacement of gadolinium in Gd[DTPA-cs124] by Tb in order to take advantage of the latter's favorable luminescent qualities (Figure 1). Since the binding affinity of DTPA-cs124 is higher for terbium than for gadolinium,[11] a response curve can be generated for the two compounds when they are mixed that is dependent on the amount of sensitized ligand in the solution (Supporting Figure 4B). This assay can be performed using a common plate reader with a time-resolved fluorescence mode.

Relaxivity and Stability Analysis. Transmetalation of the gadolinium ion is the primary concern in its clinical use, as free gadolinium has many notable effects in patients, including nephrogenic systemic fibrosis.[28] Therefore, modern-day contrast agent research focuses on the development of exceptionally stable gadolinium chelates that exhibit a high relaxivity to minimize the dose of gadolinium administered to the patient.[29] With these concerns in mind, we sought to investigate a bimodal contrast agent with increased rigidity and steric bulk to increase its overall kinetic inertness.[30] Though DTPA-cs124 was first studied and thoroughly characterized as an optical probe, it had not been explored as a potential bimodal GBCA. As such, we have investigated this complex more thoroughly within this context.[6]

r_1 of Gd[DTPA-cs124] at 60 MHz was found to be 5.09 ± 0.02 s^{-1} mM^{-1} in aqueous buffer at 37.5 °C (Table 1, Supplemental Figure 7). Gd[DTPA-cs124] was also analyzed in a competitive cation stability assay in order to compare its relative stability to those of other commercially available GBCAs. The stability index (SI) obtained from the competitive cation assay exhibited a value (SI = 0.676 ± 0.015) for Gd[DTPA-cs124] that was greater than its base structure analog gadopentetic acid (0.585 ± 0.019), as well as two other linear contrast agents, namely, gadobenic acid (0.576 ± 0.004) and gadodiamide (0.474 ± 0.029) (Figure 4, Table

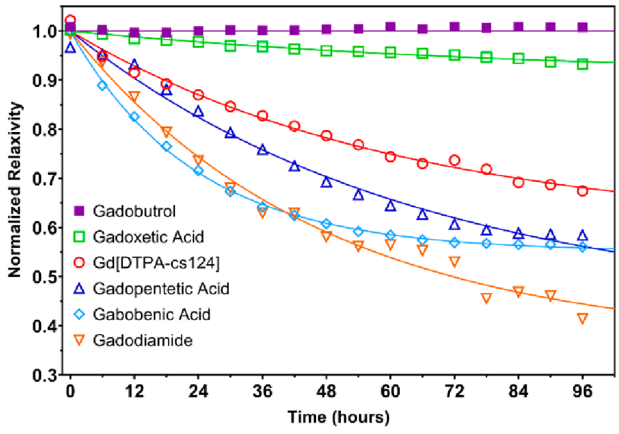

Figure 4. Competitive cation stability assay between various GBCA chelates and equimolar Zn^{2+}. Measurements acquired for gadoteric acid and gadoteridol are not featured in the plot, and exhibit highly similar trends to gadobutrol.

1). All of the macrocyclic chelators (gadobutrol, gadoteridol, and gadoteric acid), as well as gadoxetic acid, demonstrated higher stability when compared to the linear chelators, a finding that is consistent with the literature.[31,32] Similar to previous reports, a strong linear correlation between relaxivity and molecular weight was established for all of the contrast agents studied (R^2 = 0.927, p = 0.987; Table 1, Supporting

https://doi.org/10.1021/acsomega.2c05040
ACS Omega 2023, 8, 2907−2914

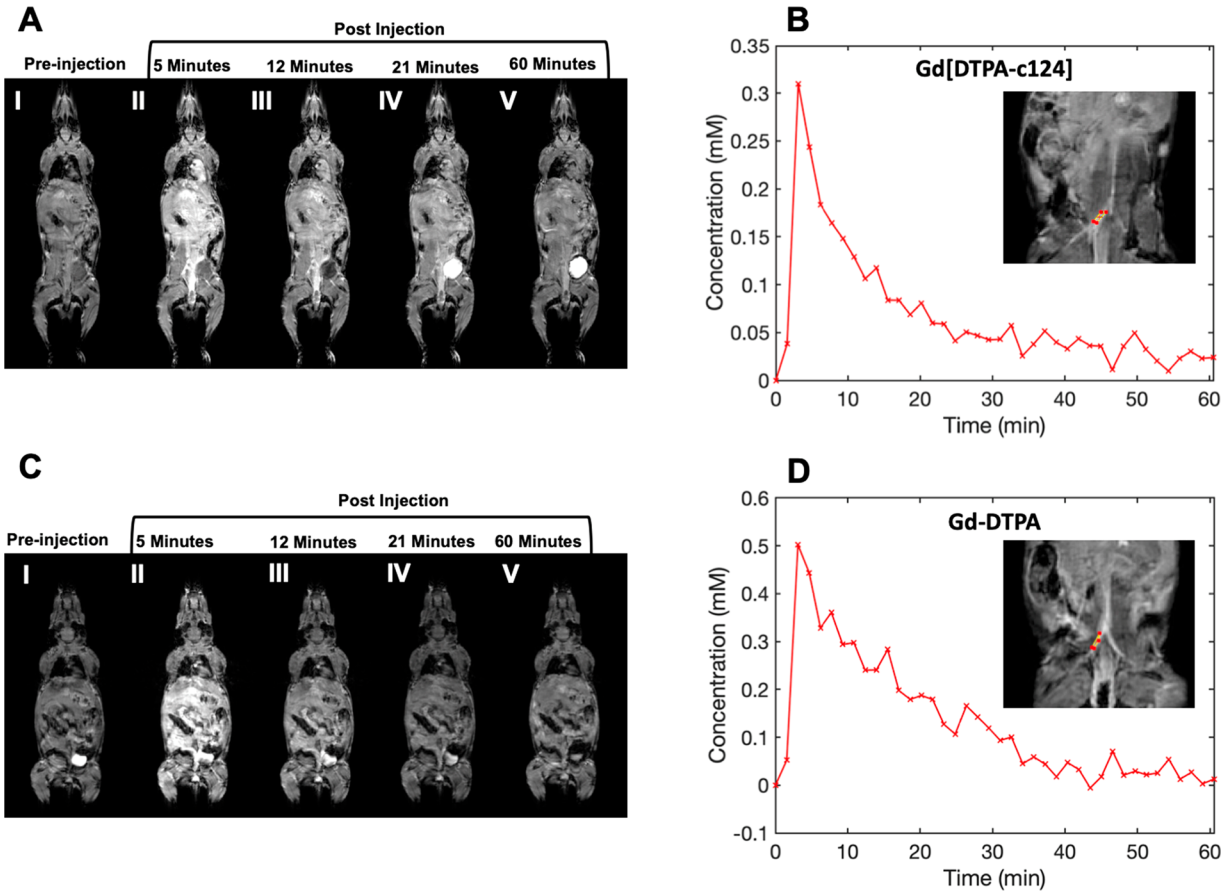

Figure 5. In vivo serial images illustrating the time course of GBCA clearance from full-body MRI scans of C57BL/6J mice (n = 3 for Gd[DTPA-cs124] and n = 1 for gadopentetic acid). (A) Horizontal 2D section covering the whole mouse from head to hindlimbs prior to and following administration of a bolus injection with Gd[DTPA-cs124] (0.1 mmol/kg) via the tail vein. (B) The corresponding time plot illustrating the contrast clearance of Gd[DTPA-cs124] monitored serially. (B, D) The absolute concentration of GBCA was obtained via a region of interest drawn within the descending aortic artery using MRI, as shown in the zoomed-in region in red. In comparison, the same time-imaging protocol and analysis was performed on a C57BL/6J mouse given an IV bolus injection of gadopentetic acid (dose = 0.1 mmol/kg). The clinically approved GBCA shows both similar (C) contrast enhancement patterns and (D) GBCA clearance, as measured using MRI via the descending aortic artery.

Figure 8).[33,34] Notably, conjugation of the fluorophore (cs124) to gadopentetic acid in order to create Gd[DTPA-cs124] increased both the stability and the relaxivity of the contrast agent compared to gadopentetic acid (Figure 5, Table 1).

In the context of linear chelators, the effect of ligand rigidity on chelate stability is best explained when comparing the relative stabilities of gadoxetic acid and gadobenic acid observed in the competitive cation assay. Both ligands of nearly identical molecular weight exhibit the same iconicity in solution and incorporate a similar moiety bound to the amine backbone of the ligand. However, their rigidity differs due to the degree of bond rotations within these moieties, where gadoxetic acid exhibits only one degree of rotation at its *para*-ethoxybenzyl moiety while gadobenic acid exhibits two. These observations and the measured relative stabilities in the competitive cation assay show that gadobenic acid has a stability mirroring that of gadopentetic acid, a chelate that can be viewed as the base structure for many clinically approved GBCAs, while gadoxetic acid exhibits the highest stability among the linear chelates. These findings suggest that the concerns regarding the stability of linear chelates may be overcome by modifying the backbone rigidity of existing clinical agents, an assertion also supported by existing literature.[30] We demonstrate the effect of increased ligand rigidity on chelate stability, given the SI of our contrast agent (0.676) when compared to that of the clinically approved analog gadopentetic acid (0.585) (Figure 4, Table 1). With our contrast agent Gd[DTPA-cs124], rigidity along the amide bond between cs124 and one of the pendant carboxylate arms not only alters the rigidity of this ligand but also decreases the overall iconicity of the complex, potentially making it less sensitive to decomplexation at lower pH compared to dianionic species such as gadopentetic acid.[30]

Given these findings, it would seem that incorporation of additional moieties would improve the stability of our chelate and, in our case, also improve the sensitivity of our assay. In this regard, the thought of utilizing Gd[DTPA$(cs124)_2$] was brought up; however, this compound had already been optically characterized and was described to have a 2.7× lower quantum yield when compared to the monoconjugate.[35] This effect was thought to be attributed to the proximity of the cs124 moieties inducing a fluorescence quenching effect, which is also observed in our assays at concentrations of DTPA-cs124 greater than 1 mM. Additionally, while the monoconjugate did show exceptional stability when compared to gadopentetic acid, we would anticipate the diconjugate to exhibit stability similar to that of gadodiamide, the GBCA observed to have the lowest stability among the featured analytes (Figure 4, Table

https://doi.org/10.1021/acsomega.2c05040
ACS Omega 2023, 8, 2907−2914

1). The addition of the cs124 moiety also increases the molecular weight of the chelate, thereby boosting its relaxivity to 5.09 mM^{-1} s^{-1} compared it to its analog gadopentetic acid, which exhibits a relaxivity of 3.83 mM^{-1} s^{-1} (Figure 4 and Table 1). This finding is consistent with the trend observed in Supplemental Figure 8 between the molecular weight and relaxivity of the contrast agent (R^2 = 0.927, p = 0.987).

In Vivo Time Course Contrast Enhancement in the Mouse Body. A set of serial 3D images of the whole mouse body were acquired using a 7T MRI in 90 min scanning sessions in order to qualitatively monitor the pharmacokinetics of Gd[DTPA-cs124] and gadopentetic acid. A 72 mm ID volume RF coil was used to uniformly cover the whole mouse body over a field-of-view (FOV) of 100 × 50 × 40 mm, enabling serial 3D T_1-weighted MR imaging with a 781 μm × 391 μm × 625 μm voxel size in less than ~2.2 min per data set. The example of 2D serial images shown (Figure 5) depict the overall abdomen of four- to six-week-old C57/BL6 mice (n = 3 for Gd[DTPA-cs124] and n = 1 for gadopentetic acid).

The selected slice level from the 3D data set was chosen to cover the different organs and anatomical regions of the mouse body. Time points from the time course depicted in Figure 5 were selected to illustrate the contrast enhancement effect of the GBCA prior to and following a single bolus injection administered with either 0.1 mmol/kg of Gd[DTPA-c124] (Figure 5A and B) or a 0.1 mmol/kg dose of gadopentetic acid (Figure 5C and D). The example of the mouse administered with Gd[DTPA-c124] exhibited successful signal enhancement and clearance in vivo, and was similar to the mouse that was administered the clinical agent, gadopentetic acid, under the same imaging conditions and an equivalent molar dose of Gd (0.1 mmol/kg).

Plasma Clearance Analysis in the Mouse. The amount of gadolinium recirculating systemically in blood following administration was sampled from a C57BL6 mouse cohort (n = 5) in rotation to minimize bias and enable quantification through the proposed PTH method. Figure 6 shows the scatter plot of gadolinium concentrations from small blood volumes sampled at different time points via 10 μL capillaries quantified using the PTH method. A two-phase decay analysis was performed to infer and compare the characteristic elimination half-lives for our proposed PTH-based method. The fast half-life of this method is 4.5 min, and the slow half-life is 105.0 min. These values agree with previously reported GBCA clearance in mice measured using Gd-153 radiolabeled gadopentetic acid, where the fast clearance half-life was measured to be between 5 and 6 min.[36] Data points that were quantified to be over 1 mM for the PTH method were excluded from the analysis in order to keep the measured values within the dynamic range of the standard curves of fluorescence.

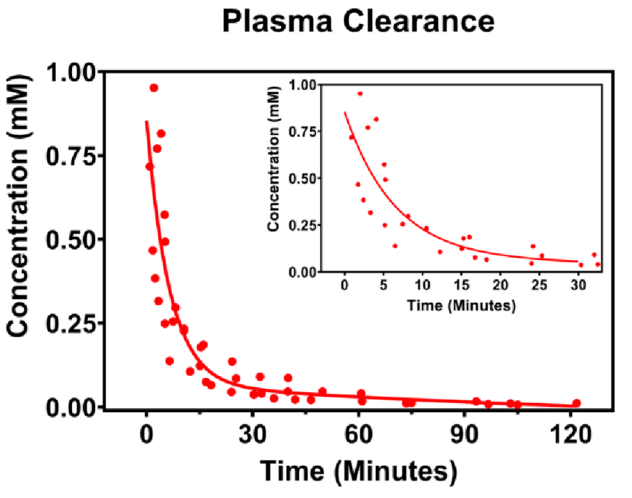

Figure 6. Scatter plot for the assessment of plasma clearance performed in C57Bl6 mice (n = 5) within 2 h of the bolus injection of the sensitized GBCA, i.e., Gd[DTPA-cs124].

Although the use of Gd[DTPA-cs124] as a bimodal GBCA is novel in this study, modern clinical MRI is predominantly performed using macrocyclic GBCAs due to their increased stability and better safety profiles.[37] While the incorporation of the fluorescent cs124 moiety has made this GBCA favorable when compared to its clinically approved analogs, its stability is still outperformed when compared to other clinically approved macrocyclic GBCAs (Figure 4, Table 1). In order to extend the application of this assay to macrocyclic chelates, our protocol will need to be adapted to include both a macrocyclic probe as well as conditions that overcome the increased kinetic stability observed in macrocyclic chelates,[30] for example, through the use of a prolonged incubation period, heat or microwave irradiation, or pH-induced transmetalation.

CONCLUSION

In conclusion, we have demonstrated that with a simple transmetalation assay utilizing a Tb salt, the concentration of a sensitized gadolinium chelate sampled from blood can be quantified through PTH using a plate reader capable of performing time-resolved fluorescence measurements. Furthermore, our proposed assay can quantify gadolinium concentrations from the subnanomolar range up to 1 mM depending on the media. Further investigation into the accuracy of this fluorescent quantification method is warranted in applications of tumor pharmacokinetic modeling in preclinical and clinical studies.[3]

FUTURE DIRECTIONS

Thanks to the small 10 μL volumes needed for our proposed assay, our approach enabled more than 35 time points to be acquired for the plasma clearance analysis from only 5 animals. This proof-of-concept study focused on a single mouse strain, the C57BL/6J strain, and would greatly benefit from additional mice in order to improve the power of analysis as well as provide further validation. Further experimentation can be done by incorporating different fluorescent moieties in place of cs124, with near-infrared (NIR) dyes being one example. Such changes may provide the added advantage of increasing the depth of signal penetration, decreasing signal attenuation, and even the possibility of in vivo imaging. In future studies, we would aim to investigate this contrast agent across a variety of rodents and mouse strains typically used in cancer models and compare the measurements against ICP-MS.

ASSOCIATED CONTENT

Supporting Information

The Supporting Information is available free of charge at https://pubs.acs.org/doi/10.1021/acsomega.2c05040.

Synthesis and physiochemical properties of DTPA-cs124; fluorescence measurement methods; results of synthesis and fluorescence measurements; HPLC

https://doi.org/10.1021/acsomega.2c05040
ACS Omega 2023, 8, 2907−2914

chromatogram and purification method; LCMS data; NMR data; concentration calibration curve and extinction coefficient of DTPA-cs124; absorption and emissions spectra of DTPA-cs124, Gd[DTPA-cs124], and Tb[DTPA-cs124]; photoluminescence decay of DTPA-cs124, Gd[DTPA-cs124], and Tb[DTPA-cs124]; Gd[DTPA-cs124] standard curve in mouse blood; relaxivity plots of featured GBCA; plot of longitudinal relaxivity as a function of molecular weight for featured GBCA; and summary of the photoluminescence quantum yields for DTPA-cs124, Gd[DTPA-cs124], Tb[DTPA-cs124], and Eu[DTPA-cs124] (PDF)

AUTHOR INFORMATION

Corresponding Author

Youssef Z. Wadghiri − *Center for Biomedical Imaging (CBI), Center for Advanced Imaging Innovation and Research (CAI2R), Department of Radiology, NYU Grossman School of Medicine, New York, New York 10016, United States;* orcid.org/0000-0001-7175-9397; Email: youssef.zaimwadghiri@nyulangone.org

Authors

James A. Tranos − *Center for Biomedical Imaging (CBI), Center for Advanced Imaging Innovation and Research (CAI2R), Department of Radiology, NYU Grossman School of Medicine, New York, New York 10016, United States;* orcid.org/0000-0002-3521-029X

Ayesha Das − *Department of Radiology, Weill Cornell Medical College, New York, New York 10065, United States;* orcid.org/0000-0001-5782-8894

Jin Zhang − *Department of Radiology, Weill Cornell Medical College, New York, New York 10065, United States;* orcid.org/0000-0003-4152-521X

Sonia Hafeez − *Center for Biomedical Imaging (CBI), Center for Advanced Imaging Innovation and Research (CAI2R), Department of Radiology, NYU Grossman School of Medicine, New York, New York 10016, United States;* orcid.org/0000-0001-8277-6766

Georgios N. Arvanitakis − *Edinburgh Instruments Ltd., Livingston EH54 7DQ Scotland, U.K.;* orcid.org/0000-0003-4554-0097

Stuart A. J. Thomson − *Edinburgh Instruments Ltd., Livingston EH54 7DQ Scotland, U.K.;* orcid.org/0000-0003-0947-9268

Suleiman Khan − *Center for Biomedical Imaging (CBI), Center for Advanced Imaging Innovation and Research (CAI2R), Department of Radiology, NYU Grossman School of Medicine, New York, New York 10016, United States;* orcid.org/0000-0001-6855-8121

Neelam Pandya − *Center for Biomedical Imaging (CBI), Center for Advanced Imaging Innovation and Research (CAI2R), Department of Radiology, NYU Grossman School of Medicine, New York, New York 10016, United States;* orcid.org/0000-0003-1897-5837

Sungheon Gene Kim − *Department of Radiology, Weill Cornell Medical College, New York, New York 10065, United States;* orcid.org/0000-0002-6288-0678

Complete contact information is available at: https://pubs.acs.org/10.1021/acsomega.2c05040

Author Contributions

[▽]J.A.T. and A.D. contributed equally. The manuscript was written through contributions of all authors.

Funding

This work was supported by the NSF-DMREF under Award no. DMR 1728858, the NSF-MRSEC Program under Award no. DMR 1420073, the NYU Shiffrin-Myers Breast Can-cer Discovery Fund, NIH/NCI R01CA160620, and the NYU CTSA grant UL1 TR000038 from the National Center for Advancing Translational Sciences, National Institutes of Health. The majority of this work was performed at the NYU Langone Health Preclinical Imaging Laboratory, a shared resource partially supported by NIH/SIG 1S10OD018337-01, the Laura and Isaac Perlmutter Cancer Center Support Grant, NIH/NCI 5P30CA016087, and the NIBIB Biomedical Technology Resource Center Grant NIH P41 EB017183.

Notes

The authors declare no competing financial interest.

ACKNOWLEDGMENTS

We would like to thank Samantha Redes, who helped maintain communication between the R&D team at Edinburgh Instruments Ltd. and our lab. We would also like to thank Nicholas Ramos, Dr. Giuseppe Carlucci, and Jairo Baquero, members of the radiochemistry lab at the NYU Grossman School of Medicine, for allowing us to use their HPLC system. Additionally, we would like to thank the members of the NYU Shared Instrument Facility, notably Dr. Chin Lin for his assistance and expertise. Furthermore, we would like to thank Nora Butler and Paramesh Karandikar for their help and interest in our project. We would also like to thank G & M for their continued love and support, as well Arman Sawhney for his artistic abilities in producing our cover art. Finally, we would like to thank the members of the laboratories of Youssef Z. Wadghiri, Sungheon Gene Kim, Dan Turnbull, and Jiangyang Zhang for their continued support and feedback during the evolution of our work.

REFERENCES

(1) Choyke, P. L.; Dwyer, A. J.; Knopp, M. V. Functional tumor imaging with dynamic contrast-enhanced magnetic resonance imaging. *J. Magn. Reson. Imaging* **2003**, *17* (5), 509−520.

(2) Ramalho, J.; Semelka, R. C.; Ramalho, M.; Nunes, R. H.; AlObaidy, M.; Castillo, M. Gadolinium-Based Contrast Agent Accumulation and Toxicity: An Update. *Am. J. Neuroradiol.* **2016**, *37* (7), 1192−1198.

(3) Bharadwaj Das, A.; Tranos, J. A.; Zhang, J.; Zaim Wadghiri, Y.; Kim, S. G. Estimation of Contrast Agent Concentration in DCE-MRI Using 2 Flip Angles. *Invest. Radiol.* **2022**, *57* (5), 343−351.

(4) Knowles, B. R.; Batchelor, P. G.; Parish, V.; Ginks, M.; Plein, S.; Razavi, R.; Schaeffter, T. Pharmacokinetic modeling of delayed gadolinium enhancement in the myocardium. *Magn. Reson. Med.* **2008**, *60* (6), 1524−1530.

(5) Harrigan, C. J.; Peters, D. C.; Gibson, C. M.; Maron, B. J.; Manning, W. J.; Maron, M. S.; Appelbaum, E. Hypertrophic cardiomyopathy: Quantification of late gadolinium enhancement with contrast-enhanced cardiovascular MR imaging. *Radiology* **2011**, *258* (1), 128−133.

(6) Li, M.; Selvin, P. R. Amine-reactive forms of a luminescent diethylenetriaminepentaacetic acid chelate of terbium and europium: Attachment to DNA and energy transfer measurements. *Bioconjug Chem.* **1997**, *8* (2), 127−132.

(7) Selvin, P. R. Principles and biophysical applications of lanthanide-based probes. *Annu. Rev. Biophys. Biomol. Struct.* **2002**, *31*, 275−302.

(8) Russell, S.; Casey, R.; Hoang, D. M.; Little, B. W.; Olmsted, P. D.; Rumschitzki, D. S.; Wadghiri, Y. Z.; Fisher, E. A. Quantification of the plasma clearance kinetics of a gadolinium-based contrast agent by photoinduced triplet harvesting. *Anal. Chem.* **2012**, *84* (19), 8106−8109.
(9) Sekar, R. B.; Periasamy, A. Fluorescence resonance energy transfer (FRET) microscopy imaging of live cell protein localizations. *J. Cell Biol.* **2003**, *160* (5), 629−633.
(10) Xiao, M.; Selvin, P. R. Quantum yields of luminescent lanthanide chelates and far-red dyes measured by resonance energy transfer. *J. Am. Chem. Soc.* **2001**, *123* (29), 7067−7073.
(11) Pallares, R. M.; An, D. D.; Tewari, P.; Wang, E. T.; Abergel, R. J. Rapid Detection of Gadolinium-Based Contrast Agents in Urine with a Chelated Europium Luminescent Probe. *ACS Sens* **2020**, *5* (5), 1281−1286.
(12) Laurent, S.; Elst, L. V.; Copoix, F.; Muller, R. N. Stability of MRI paramagnetic contrast media: A proton relaxometric protocol for transmetallation assessment. *Invest. Radiol.* **2001**, *36* (2), 115−122.
(13) Laurent, S.; Vander Elst, L.; Henoumont, C.; Muller, R. N. How to measure the transmetallation of a gadolinium complex. *Contrast Media Mol. Imaging* **2010**, *5* (6), 305−308.
(14) Werner, P.; Taupitz, M.; Schroder, L.; Schuenke, P. An NMR relaxometry approach for quantitative investigation of the trans-chelation of gadolinium ions from GBCAs to a competing macromolecular chelator. *Sci. Rep* **2021**, *11* (1), 21731.
(15) Ramalho, J.; Ramalho, M.; AlObaidy, M.; Semelka, R. C. Technical aspects of MRI signal change quantification after gadolinium-based contrast agents' administration. *Magn Reson Imaging* **2016**, *34* (10), 1355−1358.
(16) Takeshita, K.; Kinoshita, S.; Okazaki, S. Simple Method for Quantification of Gadolinium Magnetic Resonance Imaging Contrast Agents Using ESR Spectroscopy. *Chem. Pharm. Bull.* **2012**, *60* (1), 31−36.
(17) Salonia, J. A.; Gásquez, J. A.; Martinez, L. D.; Cerutti, S.; Kaplan, M.; Olsina, R. A. Inductively Coupled Plasma Optical Emission Spectrometric Determination of Gadolinium in Urine Using Flow Injection On-Line Sorption Preconcentration in a Knotted Reactor. *Instrumentation Science & Technology* **2006**, *34* (3), 305−316.
(18) Clases, D.; Sperling, M.; Karst, U. Analysis of metal-based contrast agents in medicine and the environment. *TrAC Trends in Analytical Chemistry* **2018**, *104*, 135−147.
(19) Pinto, F. G.; Junior, R. E.; Saint'Pierre, T. D. Sample Preparation for Determination of Rare Earth Elements in Geological Samples by ICP-MS: A Critical Review. *Anal. Lett.* **2012**, *45* (12), 1537−1556.
(20) Christensen, K. N.; Lee, C. U.; Hanley, M. M.; Leung, N.; Moyer, T. P.; Pittelkow, M. R. Quantification of gadolinium in fresh skin and serum samples from patients with nephrogenic systemic fibrosis. *Journal of the American Academy of Dermatology* **2011**, *64* (1), 91−96.
(21) Wilschefski, S. C.; Baxter, M. R. Inductively Coupled Plasma Mass Spectrometry: Introduction to Analytical Aspects. *Clin. Biochem. Rev.* **2019**, *40* (3), 115−133.
(22) Telgmann, L.; Holtkamp, M.; Künnemeyer, J.; Gelhard, C.; Hartmann, M.; Klose, A.; Sperling, M.; Karst, U. Simple and rapid quantification of gadolinium in urine and blood plasma samples by means of total reflection X-ray fluorescence (TXRF). *Metallomics* **2011**, *3* (10), 1035−1040.
(23) Dumont, M. F.; Hoffman, H. A.; Yoon, P. R.; Conklin, L. S.; Saha, S. R.; Paglione, J.; Sze, R. W.; Fernandes, R. Biofunctionalized gadolinium-containing prussian blue nanoparticles as multimodal molecular imaging agents. *Bioconjug Chem.* **2014**, *25* (1), 129−137.
(24) Aryal, M.; Papademetriou, I.; Zhang, Y.-Z.; Power, C.; McDannold, N.; Porter, T. MRI Monitoring and Quantification of Ultrasound-Mediated Delivery of Liposomes Dually Labeled with Gadolinium and Fluorophore through the Blood-Brain Barrier. *Ultrasound in Medicine & Biology* **2019**, *45* (7), 1733−1742.
(25) Shetty, A. N.; Pautler, R.; Ghaghada, K.; Rendon, D.; Gao, H.; Starosolski, Z.; Bhavane, R.; Patel, C.; Annapragada, A.; Yallampalli, C.; et al. A liposomal Gd contrast agent does not cross the mouse placental barrier. *Sci. Rep.* **2016**, *6*, 27863.
(26) Ren, X.; Liu, L.; Li, Y.; Dai, Q.; Zhang, M.; Jing, X. Facile preparation of gadolinium(iii) chelates functionalized carbon quantum dot-based contrast agent for magnetic resonance/fluorescence multimodal imaging. *J. Mater. Chem. B* **2014**, *2* (34), 5541−5549.
(27) Galievsky, V. A.; Stasheuski, A. S.; Krylov, S. N. Improvement of LOD in Fluorescence Detection with Spectrally Nonuniform Background by Optimization of Emission Filtering. *Anal. Chem.* **2017**, *89* (20), 11122−11128.
(28) Runge, V. M. Dechelation (Transmetalation): Consequences and Safety Concerns With the Linear Gadolinium-Based Contrast Agents, In View of Recent Health Care Rulings by the EMA (Europe), FDA (United States), and PMDA (Japan). *Invest. Radiol.* **2018**, *53* (10), 571−578.
(29) Noebauer-Huhmann, I. M.; Szomolanyi, P.; Juras, V.; Kraff, O.; Ladd, M. E.; Trattnig, S. Gadolinium-Based Magnetic Resonance Contrast Agents at 7 Tesla: In Vitro T_1 Relaxivities in Human Blood Plasma. *Invest. Radiol.* **2010**, *45* (9), 554−558.
(30) Clough, T. J.; Jiang, L.; Wong, K. L.; Long, N. J. Ligand design strategies to increase stability of gadolinium-based magnetic resonance imaging contrast agents. *Nat. Commun.* **2019**, *10* (1), 1420.
(31) Aime, S.; Anelli, P. L.; Botta, M.; Fedeli, F.; Grandi, M.; Paoli, P.; Uggeri, F. Synthesis, characterization, and 1/T1 NMRD profiles of gadolinium(III) complexes of monoamide derivatives of DOTA-like ligands. X-ray structure of the 10-[2-[[2-hydroxy-1-(hydroxymethyl) ethyl]amino]-1-[(phenylmethoxy) methyl]-2-oxoethyl]-1,4,7,10-tetraazacyclododecane-1,4,7-triacetic acid-gadolinium(III) complex. *Inorg. Chem.* **1992**, *31* (12), 2422−2428.
(32) Jacques, V.; Desreux, J. F. New Classes of MRI Contrast Agents. In *Contrast Agents I: Magnetic Resonance Imaging*; Krause, W., Ed.; Topics in Current Chemistry, Vol. *221*; Springer, 2002; pp 123−164.
(33) Margerum, L. D.; Campion, B. K.; Koo, M.; Shargill, N.; Lai, J.-J.; Marumoto, A.; Christian Sontum, P. Gadolinium(III) DO3A macrocycles and polyethylene glycol coupled to dendrimers Effect of molecular weight on physical and biological properties of macromolecular magnetic resonance imaging contrast agents. *J. Alloys Compd.* **1997**, *249* (1), 185−190.
(34) Xiong, R.; Cheng, L.; Tian, Y.; Tang, W.; Xu, K.; Yuan, Y.; Hu, A. Hyperbranched polyethylenimine based polyamine-N-oxide-carboxylate chelates of gadolinium for high relaxivity MRI contrast agents. *RSC Adv.* **2016**, *6* (33), 28063−28068.
(35) Selvin, P. R.; Jancarik, J.; Li, M.; Hung, L.-W. Crystal Structure and Spectroscopic Characterization of a Luminescent Europium Chelate. *Inorg. Chem.* **1996**, *35* (3), 700−705.
(36) Tweedle.; et al. Biodistribution of Radiolabeled, Formulated Gadopentetate, Gadoteridol, Gadoterate, and Gadodiamide in Mice and Rats. *Investigative Radiology* **1995**, *30* (6), 372−380.
(37) Kanal, E. Gadolinium based contrast agents (GBCA): Safety overview after 3 decades of clinical experience. *Magn. Reson. Imaging* **2016**, *34* (10), 1341−1345.

https://doi.org/10.1021/acsomega.2c05040
ACS Omega 2023, 8, 2907−2914